

Evaluation of Quinoxalines as Corrosion Inhibitors for Mild Steel in Acid Environment

S.Chitra^{1,*}, K.Parameswari¹, M.Vidhya¹, M.Kalishwari¹, A.Selvaraj²

¹Dept. of Chemistry, P.S.G.R. Krishnammal College for Women, Coimbatore

²Dept. of Chemistry, CBM College, Coimbatore

*E-mail: rajhree1995@rediffmail.com

Received: 27 June 2011 / Accepted: 28 August 2011 / Published: 1 October 2011

Novel Quinoxaline derivatives have been synthesised and evaluated as corrosion inhibitors for mild steel in 1M sulphuric acid by weight loss, gasometry and electrochemical techniques. Results obtained showed that they are efficient corrosion inhibitors. Tafel polarisation studies revealed that the quinoxalines were mixed type inhibitors but slightly cathodic in nature. The adsorption of all the quinoxalines on the mild steel surface from the acid solution has been found to obey Langmuir adsorption isotherm. Addition of halide ions synergistically enhanced the inhibition of the quinoxalines.

Keywords: Quinoxalines, Tafel polarisation, Impedance, adsorption isotherm, synergism.

1. INTRODUCTION

Metals generally tend to move to its original state by corrosion process. Mild steel is an alloy form of iron, which undergoes corrosion easily in acidic medium. Acidic solutions are extensively used in chemical laboratories and in several industrial processes such as acid pickling, acid cleaning, acid descaling and oil wet cleaning etc. Also mild steel is used under different conditions in chemical and allied industries for handling alkaline, acid and salt solutions. Corrosion products are formed when a metal give its electrons to the oxidising substances. This can be delayed by painting the metal or the other way of protecting the metals from corrosion is to use corrosion inhibitors. Many of the well known inhibitors are organic compounds containing nitrogen, sulphur and oxygen atom [1-5]. It has been observed that many of the organic inhibitors act by adsorption on the metal surface[6]. This phenomenon is influenced by the nature and surface charge of metal, type of aggressive medium and chemical structure of inhibitors. The adsorption of corrosion inhibitor depends mainly on physicochemical properties of the molecule such as functional groups, steric factor, molecular size,

molecular weight, molecular structure, aromaticity, electron density of the donor atoms and π - electron character of donating electrons [7-10] and also on the electronic structure of the molecules[11,12].

A review of literature reveals that no work on Quinoxaline derivatives has been reported so far as inhibitors for corrosion of mild steel in H_2SO_4 . In view of the above, an attempt was made to synthesise Quinoxaline derivatives and test their validity as corrosion inhibitors by electrochemical and non-electrochemical methods.

2. EXPERIMENTAL DETAILS

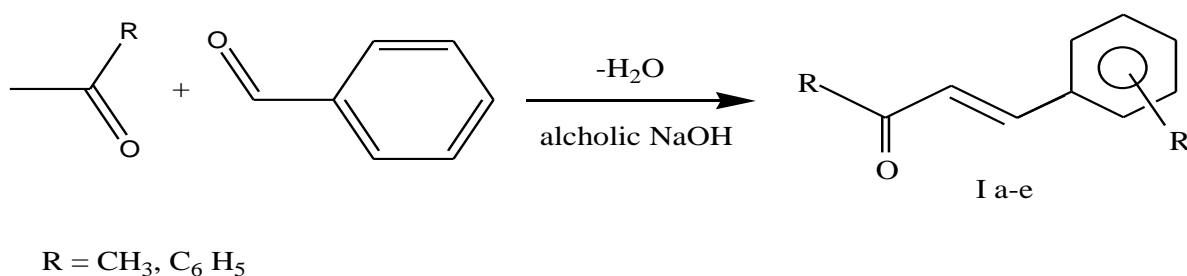
Mild steel strips containing C=0.084%, P=0.025%, Mn=0.369%, S=0.027% and the remainder iron were used for the measurement of weight loss and gasometric studies.

2.1. Synthesis of the inhibitor

Step 1 : Preparation of Chalcone

A 15 % alcoholic solution of NaOH was added in drops into a mixture containing 0.01 M aromatic aldehydes and 0.01 M acetone / acetophenone in alcohol.

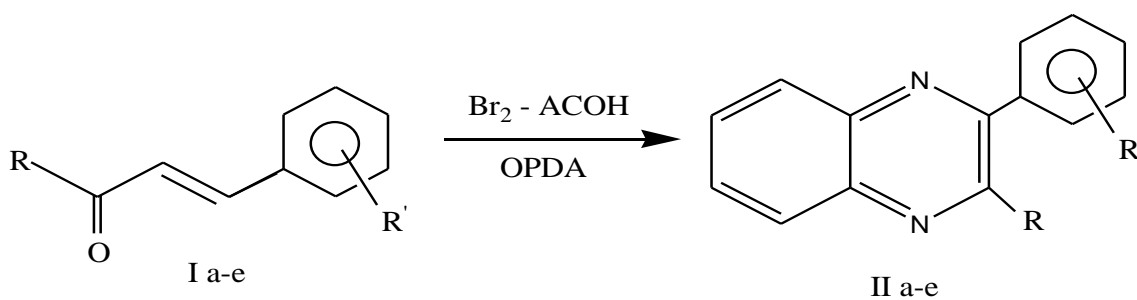
The mixture was then stirred for 3 hours, while cooling in ice and left overnight. The solid separated out (I a-e) was washed repeatedly with water and recrystallised from alcohol.



Step 2: Synthesis of Quinoxaline derivatives

To the solution of bromine in acetic acid were added the requisite chalcone, then made to react with o-phenylene diamine in sulphuric acid.

The reaction mixture was stirred for 2 hours. Then it was cooled in ice. The solid that separated out (II a-e) was collected by filtration, washed with water and recrystallised from alcohol.



Compound	R	R ¹	Name of the compound
II a	-CH ₃	-H	MPQ
II b	-C ₆ H ₅	-H	DPQ
II c	-CH ₃	-OH	MHPQ
II d	-C ₆ H ₅	-OH	PHPQ
II e	-CH ₃	-OCH ₃ , -OH	MMHPQ

Table 1. The structure of the Quinoxalines is presented in table 1.

Structure of the Compounds	
<p>3-methyl-2-phenyl quinoxaline MPQ</p>	<p>2,3-diphenyl quinoxaline DPQ</p>
<p>3-methyl-2(2'-hydroxyphenyl)quinoxaline MHPQ</p>	<p>3-phenyl-2(2'-hydroxyphenyl)quinoxaline PHPQ</p>

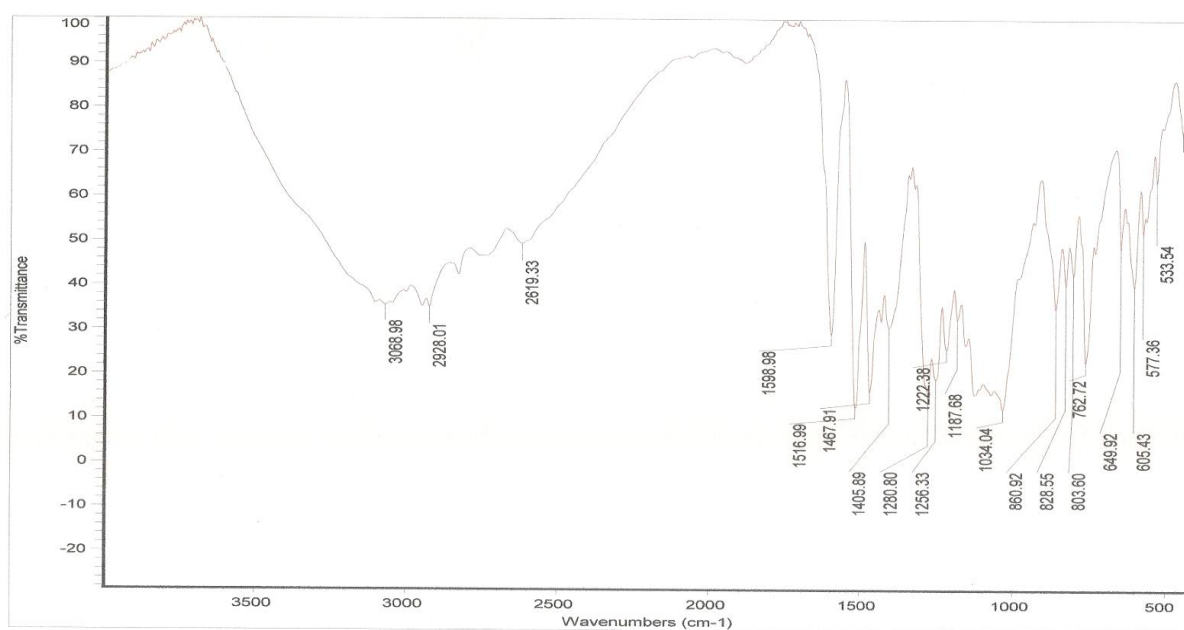
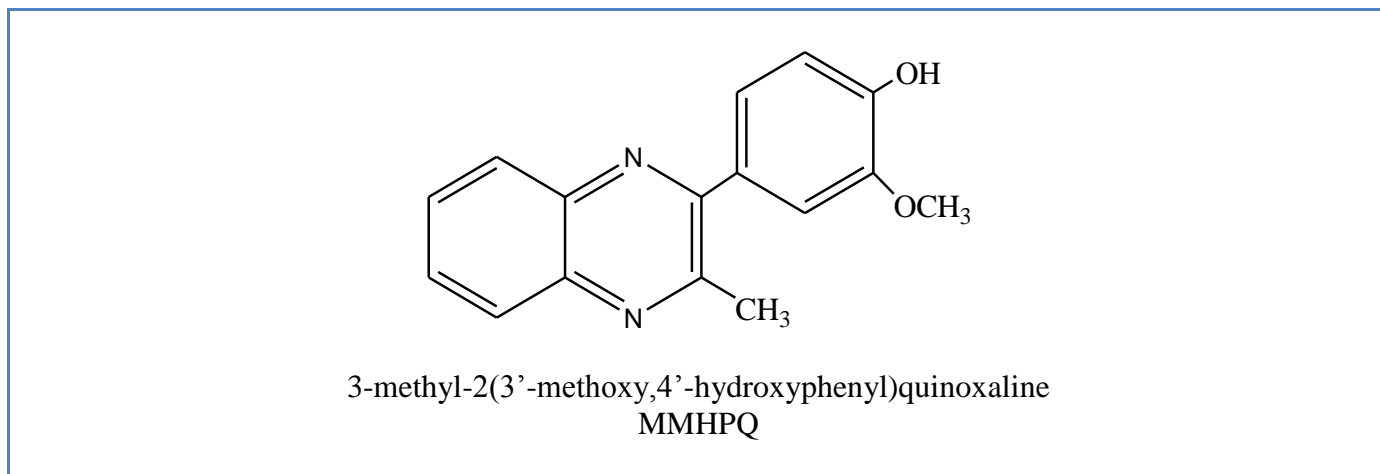


Figure 1. IR Spectrum of MMHPQ

The synthesised compounds were characterised by IR spectra. A range of techniques were used for the evaluation of inhibition efficiency.

2.2. Non-electrochemical measurements

2.2.1. Weight loss method

Mild steel specimens of size 5 cm × 2 cm × 0.05 cm were pickled with concentrated HCl. The plates were washed, dried and polished successively using emery sheets of 1/0, 2/0, 3/0 and 4/0 grades to remove adhering impurities degreased with trichloroethylene and dried using a drier. The plates were kept in a desiccator to avoid the absorption of moisture. The initial weight of the polished plate

was taken. The solutions were taken in 200 ml beakers and the specimens were suspended into the solution using glass hooks. Care was taken to ensure the complete immersion of the specimen. After a period of 3 hours the specimens were removed, washed with running water, dried and weighed using chemical balance. From the initial and final masses of the specimen (i.e. before and after immersion in the solution) the loss in weight was calculated. The experiment was repeated for various inhibitor concentrations in 1M H₂SO₄. A blank was carried out without inhibitor. Inhibition efficiency, corrosion rate and surface coverage are calculated using the following formula.

$$\text{Efficiency of inhibitor} = \frac{(\text{Weight loss without inhibitor} - \text{Weight loss with inhibitor})}{\text{Weight loss without inhibitor}} \times 100$$

$$\text{Corrosion rate (mpy)} = \frac{534 \times \text{Weight loss in mgms}}{\text{Density} \times \text{Area in sq. inch} \times \text{Time in hours}}$$

$$\text{Surface coverage}(\theta) = \frac{(\text{Weight loss without inhibitor} - \text{Weight loss with inhibitor})}{\text{Weight loss without inhibitor}}$$

From this, a graph was drawn between C/θ Vs C to know whether the adsorption of inhibitors follows Temkin / Langmuir adsorption isotherm to obtain a linear relationship.

The weight loss method was repeated at higher temperatures from 313-333K at a concentration of 1mM of the inhibitors. Activation energy (E_a), Free energy of adsorption (ΔG°), Enthalpy and entropy of activation (ΔH° & ΔS°) are calculated using the following formula.

i) Calculation of activation energy (E_a)

The activation energy was calculated by graphical method by plotting $\log(\text{corrosion rate})$ Vs $1000/T$ (K) for a temperature range of 30–60°C in 1M H₂SO₄ with and without inhibitor at a inhibitor concentration of 1mM.

$$E_a = 2.303 \times 8.314 \times \text{slope (KJ)}$$

ii) Free energy of adsorption

The free energy of adsorption $\Delta G^\circ_{\text{ads}}$ has been calculated from the equilibrium constant of adsorption using the equation.

$$k = \frac{1}{55.5} \exp \left[-\frac{\Delta G^\circ_{\text{ads}}}{RT} \right]$$

where

$$k = \frac{\theta}{C(1-\theta)} \text{ (From Langmuir equation)}$$

θ - Surface coverage of the inhibitor

C - Concentration of inhibitor in mM/200ml

$$\therefore \Delta G^\circ_{\text{ads}} = -RT \ln (55.5K)$$

iii Enthalpy and Entropy of activation ΔH° & ΔS°

Enthalpy and Entropy of activation ΔH° & ΔS° were obtained by applying the transition state equation.

$$\text{Corrosion rate CR} = \left[\frac{RT}{N_h} \right] \exp \left[\frac{\Delta S^0}{R} \right] \exp \left[\frac{\Delta H^0}{RT} \right]$$

where ‘h’ is the Planck’s constant, ‘N’ is the Avogadro number, ‘T’ is the absolute temperature and ‘R’ is the universal gas constant. A plot of $\log (CR/T)$ as a function of $1/T$ gives a straight line with slope $-\Delta H^0/R$ and intercept

$$\left[\ln \frac{R}{N_h} + \frac{\Delta S^0}{R} \right] \text{ from which the values of } \Delta H^0 \text{ \& } \Delta S^0 \text{ were calculated.}$$

2.2.2 Gasometric Technique

Mild steel specimens of size 5 cm x 2 cm x 0.05 cm were given fine mechanical polishing and degreased with trichloroethylene. The specimens were stored in a dessicator. The net area exposed was 25cm² approximately. The specimen was suspended from the hook of the glass stopper and was introduced into the cell containing 200 ml of 1M H₂SO₄. The temperature was maintained constant throughout the experiments at 303 ± 1K and at constant atmospheric pressure. Gas measurements were made for a period of an hour in all the cases. Simultaneously a duplicate was also performed in all the cases to check up the results. Experiments were repeated under identical conditions for inhibitor solution of different concentration and the gas volume was measured for duration of an hour. From the volume of hydrogen gas liberated the inhibition efficiency was calculated using the formula.

$$\text{Inhibition efficiency (\%)} = \frac{V_B - V_I}{V_B} \times 100$$

where

V_B = The volume of hydrogen evolved in the absence of inhibitor

V_I = The volume of hydrogen evolved in the presence of inhibitor.

2.3. Electrochemical studies

The mild steel rod with an exposed area of 0.785 cm^2 was polished using 1/0, 2/0, 3/0 and 4/0 emery papers and finally degreased using trichloroethylene and immediately used for the experiments. Electrochemical measurements were carried out in a glass cell with a capacity of 100 ml. A platinum electrode and a saturated calomel electrode (SEC) were used as counter electrode and a reference electrode respectively. The mild steel electrode was then placed in the test solution (uninhibited and inhibited solutions of three concentrations) for 10-15 minutes before electrochemical measurement. Electrochemical impedance spectroscopy (EIS) and Tafel polarization were conducted in an electrochemical measurement unit (Model 1280B Solartron (UK)). The EIS measurements were made at corrosion potentials over a frequency range of 10 kHz to 0.01 Hz with signals amplitude of 10 mV. The Tafel polarization measurements were made after EIS for a potential range of -200 mV to $+200 \text{ mV}$ with respect to open circuit potential, at a scan rate of 1 mV/sec . The I_{corr} , E_{corr} , R_t and C_{dl} values were obtained from the data using the corresponding “corr view” and “z view” software's.

i) Determination of inhibition efficiency by AC-impedance method

The inhibition efficiency was calculated using the formula

$$\text{Inhibition efficiency (\%)} = \frac{R_{t(\text{inh})} - R_{t(\text{blank})}}{R_{t(\text{inh})}} \times 100$$

where

$R_{t(\text{inh})}$ - Charge transfer resistance in the presence of inhibitor

$R_{t(\text{blank})}$ - Charge transfer resistance in the absence of inhibitor

ii) Determination of inhibition efficiency by potentiodynamic polarization method

The inhibition efficiency was calculated from the value of I_{corr} by using the formula.

$$\text{Inhibition efficiency (\%)} = \frac{I_{\text{corr}(\text{blank})} - I_{\text{corr}(\text{inh})}}{I_{\text{corr}(\text{blank})}} \times 100$$

where

$I_{\text{corr}(\text{blank})}$ - Corrosion current in the absence of inhibitor

$I_{\text{corr}(\text{inh})}$ - Corrosion current in the presence of inhibitor

2.4. Synergistic effect

The synergistic effect was studied by the addition of 1mM KI to the mild steel specimen immersed in 1M H₂SO₄ containing various concentrations of the inhibitors for a duration of three hours. From the weight loss data, the corrosion rate and inhibition efficiency was calculated. The same procedure was repeated by the addition of 1mM KCl and 1mM KBr.

3. RESULTS

3.1 Weight loss method

The quinoxalines were tested for nine different concentrations (0.02mM-1mM).The corrosion rate and inhibition efficiency calculated based on weight loss data are given in table 2. Table 2 reveals that inhibition efficiency increase with an increase in the concentration of the inhibitors reaching a maximum of ≈88 to 99 % at 1 mM (fig.2). Except for MHPQ & PHPQ the inhibition efficiency values reach a saturation point after 0.1 mM concentration. At the same time the corrosion rate decreases with increase in inhibitor concentration. The increase in inhibition efficiency with increase in concentration may be attributed to the increase in surface coverage (θ) by the adsorption of inhibitor on the steel surface.

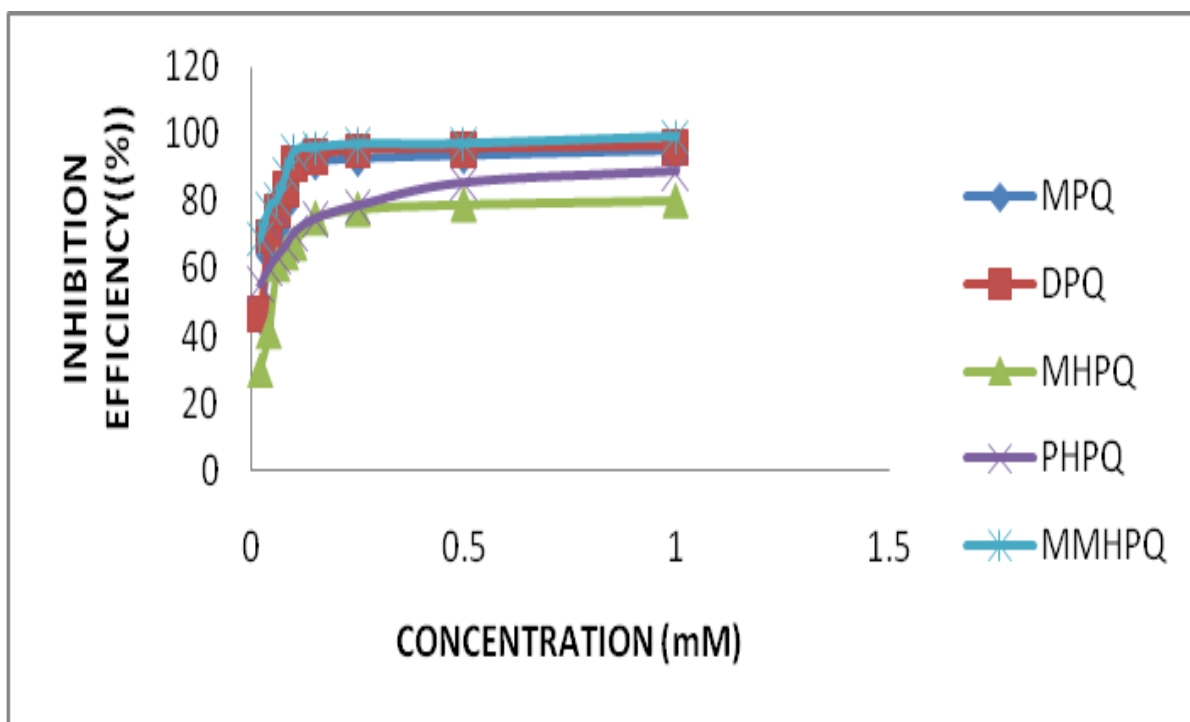


Figure 2. Plot of Inhibition efficiency (%) Vs concentration (mM) for the inhibition of corrosion of mild steel in 1M H₂SO₄

Table 2. Inhibition efficiencies of various concentrations of the inhibitors for corrosion of mild steel in 1M H₂SO₄ obtained by weight loss measurement at 30±1°C

Name of the inhibitor	Concentration (mM)	Weight loss (g)	Inhibition efficiency (%)	Degree of surface coverage (θ)	Corrosion rate (mpy)
MPQ	Blank	0.5056	-	-	-
	0.02	0.2762	45.37	0.4537	2095.14
	0.04	0.1823	63.94	0.6394	1382.85
	0.06	0.1535	69.64	0.6964	1164.38
	0.08	0.1323	73.81	0.7381	1003.57
	0.1	0.0507	89.97	0.8997	384.82
	0.15	0.0418	91.73	0.9173	317.31
	0.25	0.0381	92.73	0.9273	289.01
	0.5	0.0324	93.59	0.9359	245.77
	1	0.0248	95.09	0.9509	188.12
DPQ	Blank	0.5056	-	-	-
	0.02	0.2700	46.59	0.4659	2048.11
	0.04	0.1525	69.84	0.6984	1156.8
	0.06	0.1150	77.25	0.7725	872.34
	0.08	0.1064	78.96	0.7896	807.11
	0.1	0.0384	92.41	0.9241	291.59
	0.15	0.0373	92.62	0.9262	282.94
	0.25	0.0239	95.27	0.9527	181.3
	0.5	0.0222	95.61	0.9561	168.4
	1	0.0184	96.36	0.9636	139.57
MHPQ	Blank	0.5056	-	-	-
	0.02	0.3542	29.94	0.2994	2686.82
	0.04	0.296	41.46	0.4146	2245.33
	0.06	0.1952	61.39	0.6139	1480.7
	0.08	0.1776	64.87	0.6487	1347.2
	0.1	0.1635	67.66	0.6766	1240.2
	0.15	0.1258	75.12	0.7512	954.27
	0.25	0.1123	77.79	0.7779	851.68
	0.5	0.1053	79.17	0.7917	798.59
	1	0.0996	80.30	0.8030	755.36
PHPQ	Blank	0.5056	-	-	-
	0.02	0.2257	55.36	0.5536	1712.07
	0.04	0.1996	60.52	0.6052	1514.09
	0.06	0.1826	63.88	0.6388	1385.13
	0.08	0.1718	66.02	0.6602	1303.21
	0.1	0.1423	71.86	0.7186	1079.4
	0.15	0.1367	72.96	0.7296	1036.95
	0.25	0.1181	76.72	0.7672	895.85
	0.5	0.0733	85.50	0.8550	556.02
	1	0.0562	88.88	0.8888	426.31
MMHPQ	Blank	0.5056	-	-	-
	0.02	0.1574	68.87	0.6887	1193.97
	0.04	0.1116	77.93	0.7793	840.55
	0.06	0.0977	80.68	0.8068	741.11
	0.08	0.0599	88.15	0.8815	454.38
	0.1	0.0258	94.90	0.9490	195.71
	0.15	0.0204	95.97	0.9597	154.75
	0.25	0.0156	96.91	0.9691	118.35
	0.5	0.0150	97.03	0.9703	113.78
	1	0.0044	99.13	0.9913	33.38

3.2 Effect of temperature

The results obtained from temperature studies (40°C - 60°C) by weight loss method are shown in table 3. The data in table 3 reveal that as temperature is increased the corrosion rate increased and inhibition efficiency decreased. The decrease in inhibition efficiency with increase in temperature may be attributed to the increase in the solubility of the protective film or the reaction products precipitated on the surface of the metal that might otherwise inhibit the reaction [13]. This is in accordance with the results reported by Ergun et al [14]. The inhibition efficiency decreased drastically by ≈ 30 % at 60° C for all inhibitors.

In an acidic solution the corrosion rate is related to temperature by the Arrhenius equation

$$\log CR = \frac{-E_a}{2.303RT} + \log A \quad \text{----- (1)}$$

where ‘CR’ is the corrosion rate, ‘E_a’ is the apparent activation energy, ‘R’ is the molar gas constant, ‘T’ is the absolute temperature and ‘A’ is the frequency factor. Fig. 3 shows the plot of log CR Vs 1/T. Linear plots were obtained. The values of E_a were computed from the slope of the straight lines and are listed in table 4.

According to Dehri Ozcan[15] the relationship between temperature dependence of percent inhibition efficiency of an inhibitor and the activation energy found in its presence is given as follows.

- i) Inhibitors whose inhibition efficiency decreases with temperature increase, the value of E_a is greater than that in the uninhibited solution.
- ii) Inhibitors whose IE % does not change with temperature variation, the activation energy does not change with the presence of inhibitors.
- iii) Inhibitors whose IE % increases with temperature increase, the value of activation energy (E_a) found is less than that in the inhibited solution.

It is clear from the table 4 that E_a values in the presence of Quinoxalines are higher than that in the absence. The higher E_a values imply a slow reaction and that the reaction is very sensitive to temperature. The increase in the activation energy in the presence of Quinoxalines signifies physical adsorption [16].

The change in enthalpy (ΔH*) and entropy of activation (ΔS*) were obtained by applying the transition state equation.

$$CR = \frac{RT}{Nh} \exp \left[\frac{\Delta S^0}{R} \right] \exp \left[\frac{\Delta H^0}{R} \right] \quad \text{----- (2)}$$

where ‘h’ is Planks constant, ‘N’ is the Avogadro number, ‘T’ is the absolute temperature. Linear plots between log CR/T and 1000/T were made (fig. 3). Straight lines were obtained with the slope (-ΔH°/R) and an intercept (ln R/Nh + ΔS°/R) from which the values of ΔH° & ΔS° were calculated and listed in table 5. The more negative values of ΔH° indicate that the adsorption of the

inhibitor molecules is an exothermic reaction which implies that inhibition efficiency decreases with temperature. ΔS° values are less negative in the presence of Quinoxalines as compared to that of the blank acid, which shows that there is more disorder in the presence of inhibitors, which may be attributed to desorption of the molecules from the mild steel surface leading to randomness. But the change in entropy is greater than zero which indicates that the reaction is irreversible and complete desorption of the inhibitor is not possible.

ΔG° values calculated using the surface coverage θ (table 4) are negative indicating spontaneous adsorption of the inhibitors on the mild steel surface. But the values are within -20KJ/mole, which are consistent with the electrostatic interaction between the charged inhibitor molecules and charged metal (physical adsorption).

Table 3. Inhibition efficiencies of 1 mM concentration of various inhibitors for corrosion of mild steel in 1M H₂SO₄ obtained by weight loss measurement at higher temperature

Name of the inhibitor	Temperature (K)	Weight loss (g)	Inhibition efficiency (%)	Corrosion rate (mpy)
BLANK	303 K	0.5056	-	3835.27
	313 K	0.3029	-	6891.58
	323 K	0.4865	-	11068.8
	333 K	0.8084	-	18392.7
MPQ	303 K	0.0248	95.09	1881.22
	313 K	0.0846	72.07	1924.81
	323 K	0.234	51.09	5323.96
	333 K	0.4023	50.24	9153.1
DPQ	303 K	0.0184	96.36	1395.75
	313 K	0.0669	77.91	1522.1
	323 K	0.1487	69.36	3383.22
	333 K	0.2901	64.11	6600.33
MHPQ	303 K	0.0996	80.30	755.36
	313 K	0.1173	61.27	2668.8
	323 K	0.2706	44.37	6156.69
	333 K	0.4800	40.62	10920.92
PHPQ	303 K	0.0562	88.88	426.31
	313 K	0.0682	77.48	1551.68
	323 K	0.2475	49.12	5631.12
	333 K	0.413	48.91	9396.5
MMHPQ	303 K	0.0044	99.13	33.38
	313 K	0.0367	87.88	834.99
	323 K	0.1353	72.18	3078.3
	333 K	0.2323	71.26	5285.28

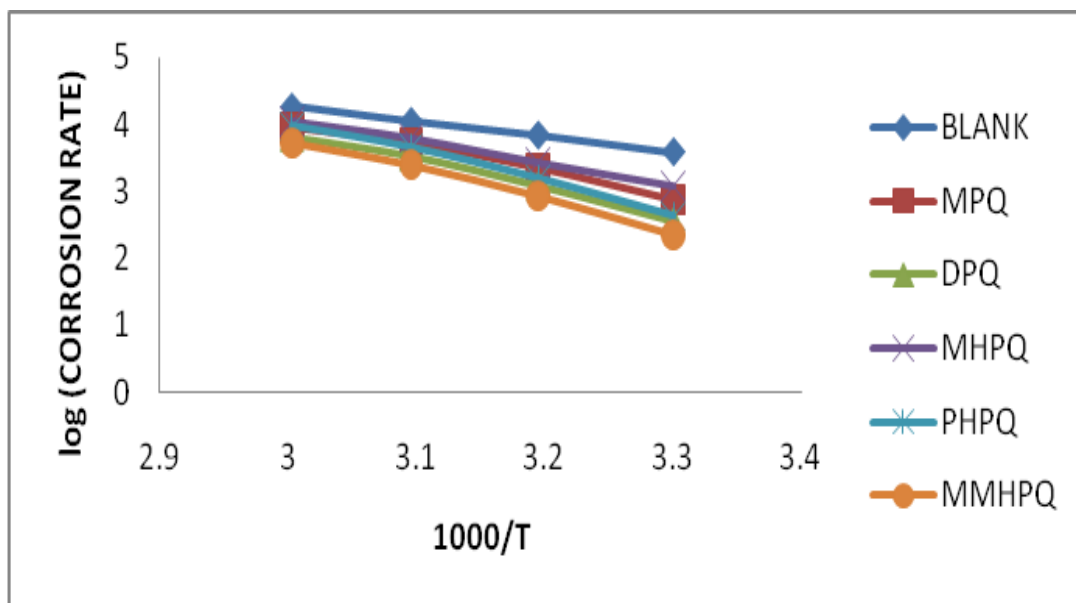


Figure 3. Arrhenius plot of corrosion of mild steel in 1M H₂SO₄ solution in the absence and presence of inhibitors

Table 4. Activation energies (E_a) and free energy of adsorption (ΔG°_{ads}) for the corrosion of mild steel in 1M H₂SO₄ at 1 mM concentration of the inhibitors

Name of the inhibitor	E _a (KJ)	ΔG° _{ads} at various temperatures (KJ)			
		303 K	313 K	323 K	333 K
BLANK	43.44	-	-	-	-
MPQ	71.13	-17.59	-12.95	-6.67	-11.15
DPQ	82.76	-18.37	-13.73	-12.99	-12.73
MHPQ	62.75	-13.66	-11.65	-10.18	-10.07
PHPQ	86.99	-15.56	-13.67	-10.69	-11.00
MMHPQ	91.12	-18.95	-15.61	-13.35	-13.63

Table 5. Kinetic/Thermodynamic Parameters for mild steel corrosion in 1M H₂SO₄

Name of the Inhibitor	E _a KJ/mole	-ΔH° KJ/mole	-ΔS° KJ/mole
BLANK	0.04080	0.01772	0.1299
MPQ	0.04195	0.01822	0.1310
DPQ	0.06648	0.02887	0.1999
MHPQ	0.06602	0.02867	0.1986
PHPQ	0.08434	0.03662	0.1752
MMHPQ	0.1059	0.04600	0.1491

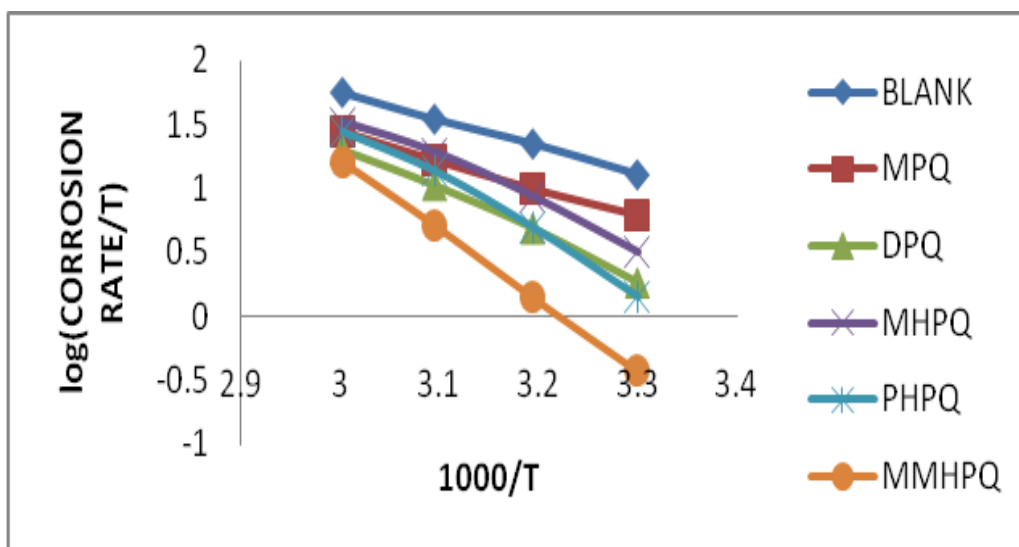


Figure 4. Transition state plot for mild steel corrosion in 1M H₂SO₄ in the absence and presence of 1mM concentration of the inhibitors

3.3 Adsorption Isotherm

Adsorption isotherms are very important in understanding the mechanism of inhibition of corrosion reaction. The most frequently used adsorption isotherms are Frumkin, Temkin, Freundlich, Florry Huggins, Bockris-swinkel, El-Awardy and Langmuir isotherms. All these isotherms can be represented as follows.

$$f(\theta,x)\exp(-2a\theta)=KC \text{ -----(3)}$$

where $f(\theta,x)$ is the configuration factor which depend upon the physical model and the assumptions underlying the derivation of the isotherm. ‘ θ ’ is the degree of surface coverage , ‘ c ’ is the inhibitor concentration in the electrolyte, ‘ x ’ is the size ratio , ‘ a ’ is the molecular interaction parameter and ‘ k ’ is the equilibrium constant of the adsorption process.

Adsorption behaviour of Quinoxalines is best explained by Langmiur isotherm. Langmiur isotherm is an ideal isotherm for physical or chemical adsorption where there is no interaction between the adsorbate and the adsorbent[17].Assumption of Langmiur relate the concentration of the adsorbate in the bulk of the electrolyte (C) to the degree of surface coverage (θ) according to the equation.

$$\frac{C}{\theta} = \frac{1}{K} + C \text{ ----- (4)}$$

where ‘ k ’ is the equilibrium constant of adsorption. Taking log on both sides of equation (4).

$$\log C/\theta = \log C - \log K \text{ ----- (5)}$$

By plotting values of ‘ C/θ ’ Vs values of ‘ C ’, straight line graph were obtained (fig.5).

Applicability of Langmuir adsorption isotherm to the adsorption of Quinoxalines on mild steel confirms the formation of multimolecular layer of adsorption where there is no interaction between the adsorbate and the adsorbent.

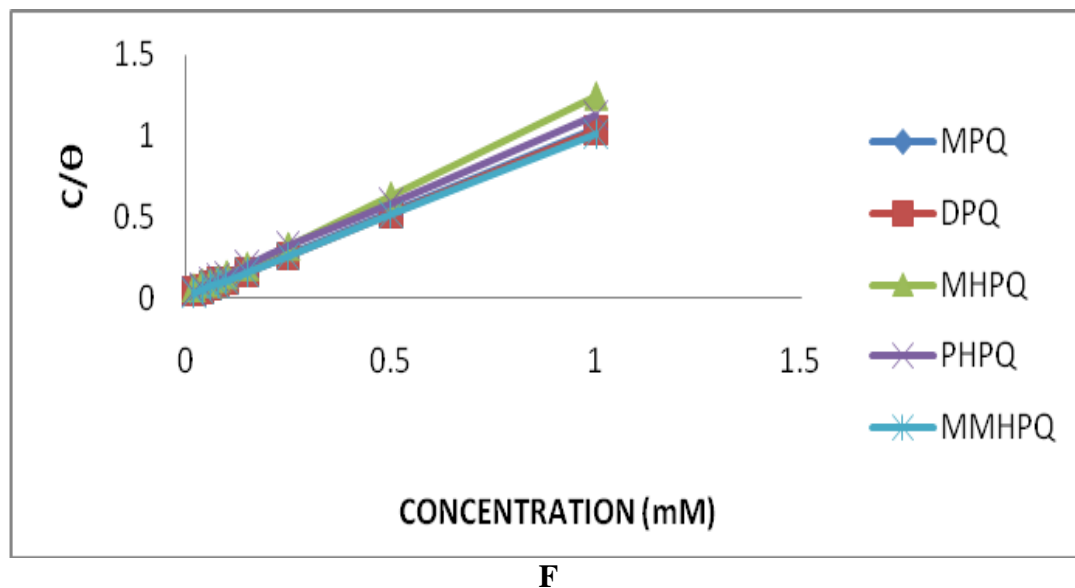


figure 5. Langmuir plot of inhibitors in 1M H₂SO₄

3.4 Gasometry

Table 6. Inhibition efficiencies for the selected concentrations of the inhibitors for the corrosion of mild steel in 1M H₂SO₄ obtained by gasometric measurement

Name of the inhibitor	Concentration (mM)	Volume of gas (cc)	Inhibition efficiency (%)
Blank		26.4	-
MPQ	0.02	13.7	48.18
	0.1	4.7	82.20
	1	1.2	95.45
DPQ	0.02	14.4	45.45
	0.1	1.9	92.80
	1	1.1	95.83
MHPQ	0.02	19.5	26.13
	0.1	9.2	65.15
	1	2.6	90.15
PHPQ	0.02	12.1	54.17
	0.1	7.4	71.97
	1	3.4	87.12
MMHPQ	0.02	8.7	67.05
	0.1	1.4	94.67
	1	0.2	99.24

The corrosion rate of mild steel and the inhibition by Quinoxalines in 1M H₂SO₄ were assessed by the volumetric measurements of the evolved H₂ gas when the specimen was immersed in H₂SO₄. Addition of inhibitors into the corrosive resulted in a reduction in the volume of the H₂ gas evolution. The results are shown in the table 6. The inhibition efficiency increases with increase in concentration and the obtained results agree with the weight loss measurements.

3.5 Polarisation studies

Potentiodynamic polarisation curves for mild steel in 1M H₂SO₄ are shown in figure 6. The polarization parameters E_{corr}, I_{corr}, Tafel (b_a, b_c) and inhibition efficiency are listed in table 7. The lower corrosion current density (I_{corr}) values in the presence of inhibitors without causing significant changes in corrosion potential (E_{corr}) suggest that the compound is mixed type inhibitor and are adsorbed on the surface there by blocking the corrosion reaction. The 'b_a' value are shifted to a larger extent than 'b_c' values, suggesting that though the inhibition is under mixed control, the effect of the inhibitor on the anodic polarization is more pronounced than on the cathodic polarization.

Table 7. Corrosion parameters for corrosion of mild steel with selected concentrations of the inhibitors in 1M H₂SO₄ by potentiodynamic polarization method

Name of the inhibitor	Concentration	Tafel slopes (mV/dec)		E _{corr} (mV)	I _{corr} (μAmp/cm ²)	Inhibition efficiency (%)
		b _a	b _c			
Blank		150.034	158.506	-0.4840	1725.0	-
MPQ	0.02	63.552	169.59	-0.4856	110.02	93.62
	0.1	58.237	189.14	-0.4841	78.95	95.42
	1	55.684	179.32	-0.4816	56.375	96.73
DPQ	0.02	44.109	190.30	-0.4869	105.28	93.90
	0.1	39.444	188.18	-0.4816	97.285	94.36
	1	36.148	194.76	-0.4675	37.834	97.81
MHPQ	0.02	70.268	191.84	-0.4788	214.08	87.59
	0.1	68.011	175.55	-0.4857	177.48	89.71
	1	65.859	170.95	-0.4884	120.00	93.04
PHPQ	0.02	43.398	185.47	-0.4849	123.74	92.82
	0.1	39.357	138.19	-0.4805	91.729	94.68
	1	40.459	180.21	-0.4692	83.224	95.18
MMHPQ	0.02	71.222	187.63	-0.4852	486.55	89.19
	0.1	51.489	194.37	-0.4824	35.442	97.95
	1	68.347	167.25	-0.4863	15.945	99.08

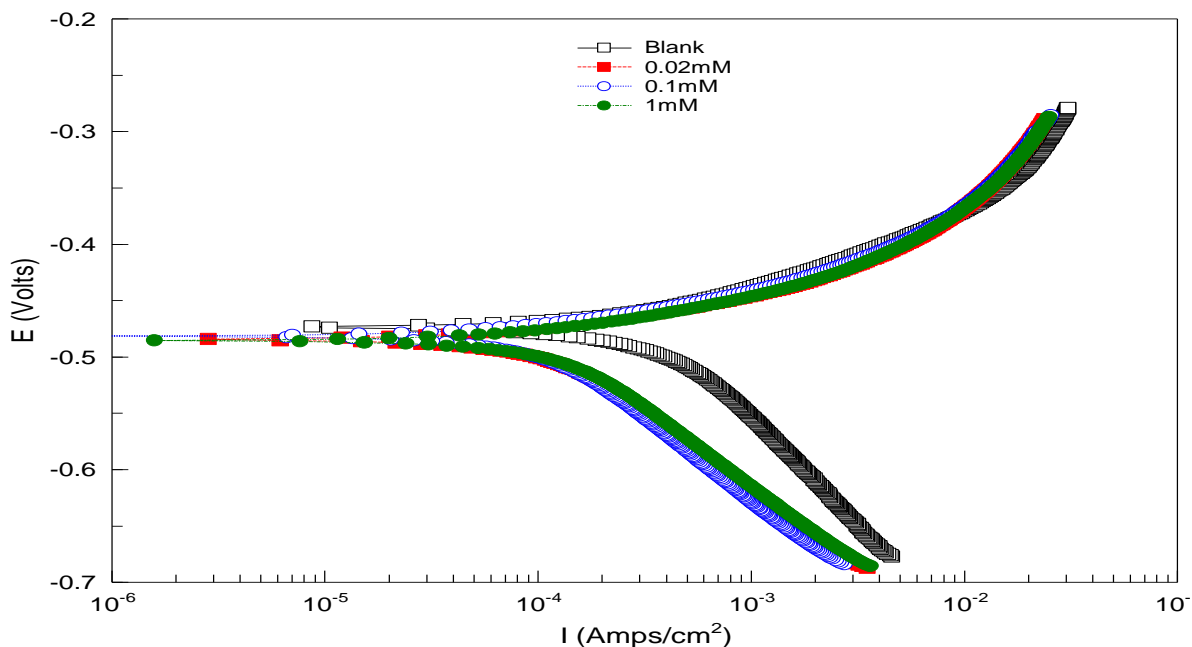


Figure 6. Polarization curves for mild steel in 1M H₂SO₄ for selected concentrations of inhibitor MMHPQ

3.6 Electrochemical impedance spectroscopy studies

Table 8. AC-impedance parameters for corrosion of mild steel for selected concentrations of the inhibitors in 1M H₂SO₄

Name of the inhibitor	Concentration (mM)	R _t (ohm cm ²)	C _{dl} (μF/cm ²)	Inhibition efficiency (%)
Blank		10.5299	34.2381	-
MPQ	0.02	99.89	19.057	89.46
	0.1	134.21	18.328	92.15
	1	148.44	15.774	92.91
DPQ	0.02	116.23	10.354	90.94
	0.1	150.54	10.137	93.01
	1	203.17	10.086	94.81
MHPQ	0.02	126.07	18.113	91.65
	0.1	130.38	17.454	91.92
	1	139.69	17.286	92.46
PHPQ	0.02	110.86	23.195	90.50
	0.1	127.31	22.539	91.73
	1	146.74	18.431	92.82
MMHPQ	0.02	116.20	16.627	90.94
	0.1	321.79	6.6883	96.73
	1	325.51	4.2546	96.77

Impedance diagram (Nyquist plot) obtained for mild steel in 1M H₂SO₄ in the presence of selected concentrations of the inhibitors are depicted in figure 7. They are perfect semicircles and this may be attributed to the charge transfer reaction. Impedance parameters derived from Nyquist plots are tabulated in table 8. From the table it is evident that as the concentration of the inhibitor increases, C_{dl} values decrease and R_t values increase. Decrease in C_{dl} is due to an increase in the thickness of the electrical double layer. This suggests that the inhibitor molecules function by adsorption at the metal-solution interface.

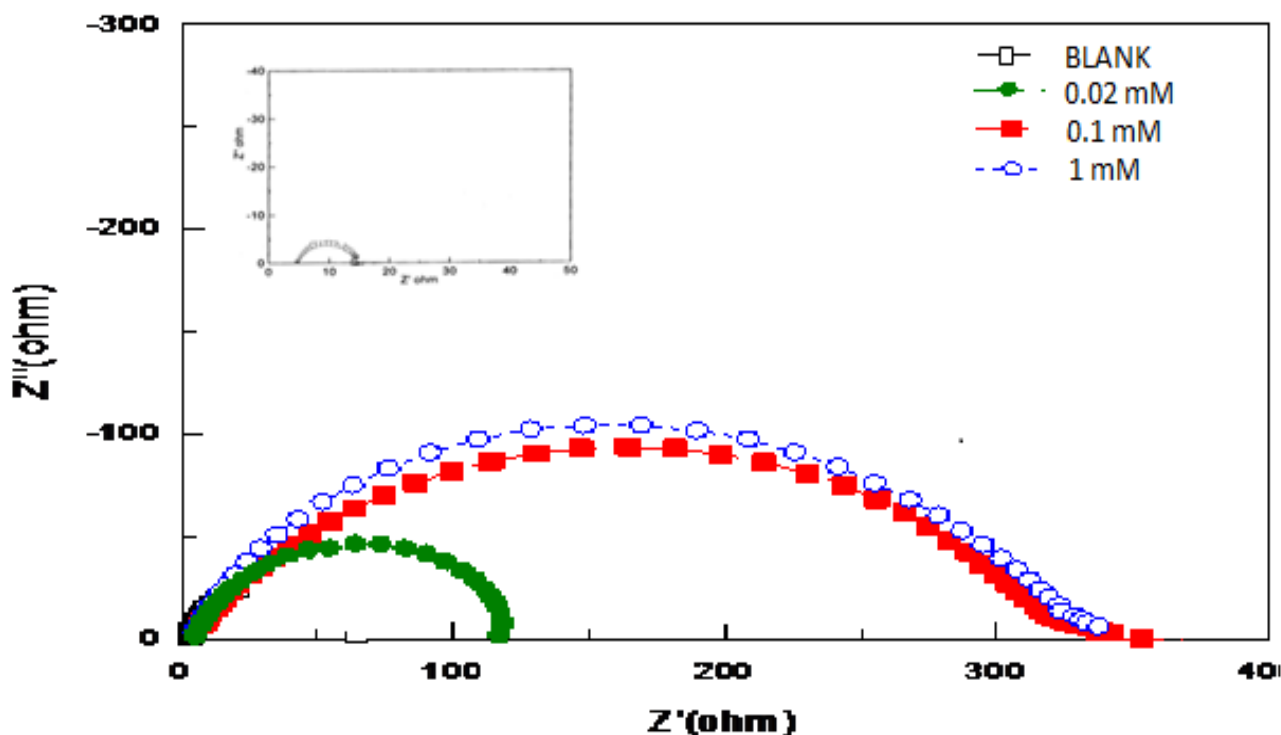


Figure 7. Nyquist diagram for mild steel in 1M H₂SO₄ for the selected concentrations of inhibitor MMHPQ

3.7 Synergistic effect of halide ion

It is well known that nitrogen based organic compounds are effective inhibitors for mild steel corrosion in aqueous solution. The presence of lone pair of electrons on the nitrogen atoms and π -electrons of aromatic ring facilitate their adsorption on the metal surface by interaction with the vacant d-orbital of iron. Heterocyclic compounds may also be adsorbed through electrostatic interactions between positively charged nitrogen atom and the negatively charged metal surface.

It is also known that adsorption of an inhibitor can be influenced by the nature of the anions in acidic solutions. The presence of halide ions is found to enhance the inhibition efficiency. They are characterized by their strong adsorbability on the metal surface which brings about a negative charge favouring the adsorption of the cation type inhibitors.

The Quinoxalines contain 2 nitrogen atoms in the ring system and these compounds get transformed into cations in acid solution. Therefore the inhibition efficiency of the quinoxalines can be enhanced by the presence of halide ions. Hence an attempt has been made to study the influence of added halides by weight loss method.

The values of inhibition efficiency in the presence of 1 mM KCl, KBr and KI in 1M H₂SO₄ at various concentrations of the inhibitors is presented in table 9. The inhibition efficiency increases in the presence of halide ions at all concentrations of the inhibitors studied. This may be attributed to the strong chemisorption of halide ions. The cationic inhibitor molecules are then adsorbed on the metal surface by coulombic attraction to the adsorbed halide ions on the metal surface. The process is similar to the anion-induced adsorption as reported by Oguzie et al [18].

The synergistic effect was observed to increase in the order Cl⁻ < Br⁻ < I⁻. The trend is suggestive of a possible role played by the radii and electronegativities of the halide ions. Electronegativity decreases from Cl⁻ to I⁻ and ionic radii increases in the order of Cl⁻ < Br⁻ < I⁻. This suggests that the iodide ion radius is more predisposed to adsorption than Br⁻ and Cl⁻.

Table 9. Synergistic effect of 1mM KCl / KBr / KI on the inhibition efficiency of inhibitors by weight loss method at 30±1°C

Name of the inhibitor	Concentration (mM)	Inhibition efficiency (%)			
		Without KCl, KBr and KI	With 1mM KCl	With 1mM KBr	With 1mM KI
MPQ	0.02	45.37	56.13	74.30	96.72
	0.06	69.64	76.48	82.90	97.09
	0.1	89.97	92.15	94.48	99.18
DPQ	0.02	46.59	60.03	79.68	92.54
	0.06	77.25	80.15	85.32	93.19
	0.1	92.41	93.39	95.60	99.37
MHPQ	0.02	29.94	49.74	65.39	95.61
	0.06	61.39	73.48	75.66	96.32
	0.1	67.66	74.88	80.91	97.10
PHPQ	0.02	55.36	60.11	69.90	84.71
	0.06	63.88	65.88	74.49	97.63
	0.1	71.86	75.50	84.79	98.95
MMHPQ	0.02	68.87	73.75	83.61	98.53
	0.06	80.68	89.29	90.80	99.30
	0.1	94.90	95.32	96.69	99.59

3.8 Surface analysis

The mild steel specimens immersed in the blank acid (1M H₂SO₄) and inhibited acid (1mM inhibitor) were observed under an optical microscope (OLYMPUS BX51M) and the photomicrographs are shown in the figure 8. The photographs show that the mild steel is heavily corroded in 1M H₂SO₄ whereas in the presence of inhibitor in acid, the surface condition is comparatively better. This suggests

the presence of a protective adsorbed layer of the inhibitor on the mild steel surface which impedes corrosion rate of the metal appreciably.

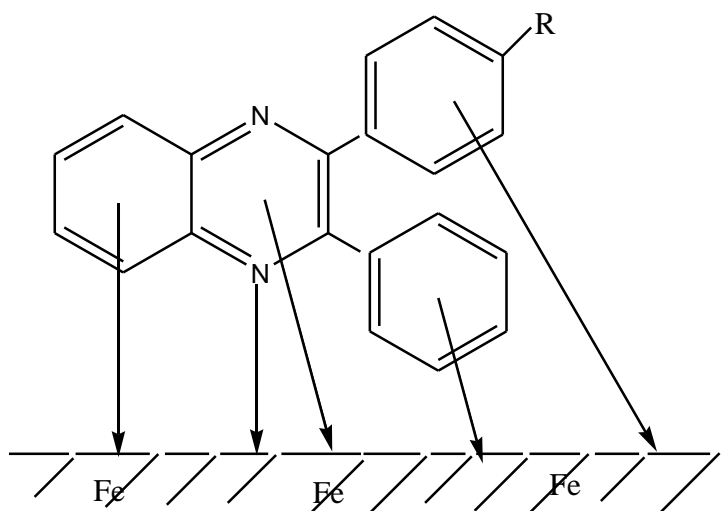


Figure 8. Optical Microscope images of mild steel surface without and with the addition of MMHPQ

4. DISCUSSION

4.1 Mechanism of corrosion inhibition

The organic compounds containing S, N and O are known to be effective inhibitors. Its effectiveness depends on the electron density of the functional groups.



4.2 Evaluation of inhibitors

The order of inhibition efficiency of the synthesised Quinoxalines is
MMHPQ > DPQ > MPQ > PHPQ > MHPQ

The corrosion inhibition property of the Quinoxalines can be attributed to the presence of hetero atom and π -electrons on benzene ring. These factors play a vital role in the adsorption of the inhibitor. The adsorption of the inhibitor on the steel surface can occur either directly by the

interactions between the π -electrons of the inhibitor and the vacant 'd' orbitals of metal surface atoms. There may also be an interaction of the inhibitor with adsorbed sulphate ions which lead to the adsorption of inhibitor [19,20]. The adsorption of the inhibitor on mild steel may also be due to the interaction of the lone pair of electrons on 'N' with the surface atoms of the metal. All the above interactions cause the adsorption of Quinoxalines on corroding the sites of the metal and prevent the anodic reaction. As inhibitor concentration increases, it covers more and more surface area and results in reduction of corrosion rate. All the five inhibitors exhibit a maximum inhibition efficiency of 80 to 98% at a concentration of 1mM. Their inhibition efficiency may be due to the presence of 2/3 benzene rings with one containing 2 'N' atoms. The π -electrons of the benzene ring and the lone pair of electrons on nitrogen act as anchoring sites for adsorption. MMPHQ exhibit a maximum inhibition efficiency of about 98% which is slightly higher than DPQ and MPQ. This may be due to the presence of the $-\text{OCH}_3$ and $-\text{OH}$ substituents in the phenyl ring which increase the electron density of the benzene ring and thereby enhance adsorption i.e., they act as additional anchoring sites for adsorption. DPQ has slightly high inhibition efficiency than MPQ due to the presence of an extra phenyl ring. PHPQ and MHPQ are expected to be more efficient inhibitors than DPQ and MPQ, but their inhibition efficiency values are ≈ 80 -88 %. This decrease in inhibition efficiency may be attributed to the greater solubility of the hydroxy compound in aqueous acid medium leading to the dissolution of the inhibitor film from the metal surface. This is in accordance to the findings of Quraishi et al [21].

5. CONCLUSION

The conclusions arrived based on the investigations are

➤ The order of inhibition efficiency of the synthesized compounds at 1 mM concentration is

MMHPQ > DPQ > MPQ > PHPQ > MHPQ

➤ All investigated inhibitors are effective inhibitors for corrosion of mild steel in 1M H_2SO_4 and for copper in 1M HNO_3 .

➤ The inhibition efficiency increases with increase in inhibitor concentration.

➤ They inhibit corrosion by getting adsorbed on the metal surface.

➤ The adsorption of inhibitors follows Langmuir adsorption isotherm.

➤ The effect of temperature indicates that the inhibition efficiency decreases with rise in temperature.

➤ The activation energy (E_a) is higher for inhibited acids than for uninhibited acids showing the temperature dependence of inhibition efficiency.

➤ The less negative values of $\Delta G^\circ_{\text{ads}}$ with increase in temperature indicate the spontaneous adsorption of the inhibitors on the metal surface.

➤ Electrochemical impedance spectroscopy experiments have shown that an increase in inhibitor concentration causes an increase in charge transfer resistance R_t and a decrease in C_{dl} value, owing to the increased thickness of the adsorbed layer.

- The Tafel slopes obtained from potentiodynamic polarization curves indicate that all the inhibitors behave as mixed type inhibitors but anodic effect is more pronounced.
- Addition of halide ions to the inhibitors shows an increase in inhibition efficiency. The synergistic influence of halide ion follows the order $I^- > Br^- > Cl^-$

References

1. K.C Emregul and Atakol, *Mater. Chem.Phys.*, 82, (2003), 188.
2. S.N Raicheva, B.V.Aleksiev and E.I.Sokolova, *Corro.Sci.*, 34,(1993),343.
3. S.Arab and E.A Noor, *Corrosion* , 49,(1993),122.
4. A.Sayed El, *J.Appl.Electrochem.*, 27,(1997),193.
5. X.L.Cheg, H.Y.Ma, S.chen,R.Yu,X.Chen,X.M.Yao, *Corros.Sci.*,41,(1993),321.
6. S.S.Abdel Rehim, M.A.M.Ibrahim and K.F.Khaled, *J.Appl.Electrochem.*, 29,(1999), 593. 7.
7. E.Khamis, *Corrosion*,46,(1990),476.
8. E.Stupnisek Lisac and S.Podbrscek, *J.Appl.Electrochem.*, 24,(1994),779.
9. I.L.Rosenfeld, *Corrosion Inhibitors* –Mc Graw-Hill, Newyork,(1981).
10. E.Stupnisek Lisac and M.Metikos-Hukovic, *Br.corros.J.* ,28,(1993),74.
11. S.L.Granese, B.M.Rosales, C.Oviedo and J.O.Zerbino, *Corros.sci.*,33,(1992), 1439.
12. S.L.Granese, *Corrosion*, 44,(1988),322.
13. E.E.Ebenso, Hailemichael Alemu, S.A.Umoren and I.B.Obot, *Int.J.Electrochem.Sci.*, 3(2008),1325.
14. U.Ergun,D.Yuzer, K.C.Emergul, *Mater. Chem.Phy.*,109,(2008), 492.
15. I.Decri, M.Ozcan, *Mater. Chem.Phy.*, 98,(2006), 316.
16. M.I.Awad, *J.Appl.Electrochem.*, 36,(2006), 1163.
17. D.S.Sheatty, P.Shetty, H.V.S.Nayak, *J.of Chilean Chem.Soc.*, 51,(2006),849.
18. E.E. Oguzie, C.Unaegbu, C. N. Ogukwe, A.I. Onuchukwu, *Mater.Chem.Phy.*, 84,(2004),363.
19. N.Hackerman, E.S. Snavely and J.S.Payne, *J.Electrochem. Soc.*, 113,(1966),667.
20. T.Murakawa,S.Nagaura and N.Hackerman, *Corros.Sci.*, 7, (1967),79.
21. M.A.Quraishi, S.Muralidharn and S.V.K.Iyer, *Corros.Sci.*,37,(1995),1739.